frontiers | Frontiers in Materials

TYPE Original Research
PUBLISHED 10 January 2025
DOI 10.3389/fmats.2024.1514559

OPEN ACCESS

EDITED BY
Richard Drevet,
Masaryk University, Czechia

REVIEWED BY
Dapeng Li,
University of Massachusetts Dartmouth, United States
Josefina Ballarre,
National Scientific and Technical Research Council (CONICET), Argentina

*CORRESPONDENCE
Geetha Balasubramani,
geethapriya1728@gmail.com

RECEIVED 21 October 2024
ACCEPTED 26 November 2024
PUBLISHED 10 January 2025

CITATION
Balasubramani G, J. P and J. PP (2025) Optimizing bone-metal implant interfaces: the role of bio-ceramic coatings in improving stability and tissue metabolism.
Front. Mater. 11:1514559.
doi: 10.3389/fmats.2024.1514559

Optimizing bone-metal implant interfaces: the role of bio-ceramic coatings in improving stability and tissue metabolism

Geetha Balasubramani[1]*, Premkumar J.[1] and Paul Pradeep J.[2]

[1]Department of Biomedical Engineering, School of Bio and Chemical Engineering, Sathyabama Institute of Science and Technology, Chennai, India, [2]MedCuore Medical Solutions Private Limited, Chennai, India

Introduction: Bone replacement is often necessary for patients experiencing pain or swelling in the knee or limb bone region due to osteoarthritis and other bone- related diseases. During surgery, a new bone implant made of metal-on-metal (titanium, cobalt-chromium) or polymer-on-metal (polyethylene on titanium) is used. A significant drawback of these implants is the accumulation of metal or polymer debris, leading to inflammation and infections. Infections or inflammation caused by bacterial adherence to the implant surface result in biofilm formation at the implantation site. Additionally, infections can arise from metal debris generated by the friction and movement of the knee joint, known as implant-associated infections.

Methods: This research aims to develop a bio-ceramic- based composite coating for metal implants. The composite comprises beta- tricalcium phosphate, pectin, gelatine, and polyvinylpyrrolidone (PVP) applied to a 12 mm cortical titanium screw. This coating is designed to enhance the biocompatibility, antibacterial properties, and anti-inflammatory activities of the bone screw, promoting cell growth around the implant and creating a viable environment at the implantation site.

Results and Discussion: Primary characterization of the composite coating materials was conducted using Scanning Electron Microscopy (SEM) with Energy Dispersive X-ray (EDX) analysis and Fourier Infrared Spectroscopy (FTIR). *In-vitro* antibacterial testing, anti-inflammatory testing, and degradation.

KEYWORDS

bone implants, dip coating, cortical screw, tissue engineering, antibac terial property

1 Introduction

Bone replacement surgeries, such as total knee arthroplasty (TKA) and total hip arthroplasty (THA), are vital interventions to restore joint function in patients suffering from severe osteoarthritis, trauma, or degenerative bone diseases. These procedures involve the replacement of damaged bone with artificial implants that replicate the structure and function of natural bone. Despite significant advancements in implant

technology, complications such as implant instability, poor osseointegration, and post-surgical infections persist, impacting long-term clinical outcomes (Albrektsson et al., 1981). Reports indicate that instability issues affect up to 20% of total knee replacements, often necessitating revision surgeries and prolonging patient recovery (Albrektsson et al., 1981; Bello et al., 2020). Additionally, implant-associated infections (IAIs) pose a considerable risk, with incidence rates ranging from 1%–5% in primary arthroplasties and up to 30% in trauma-related procedures, significantly compromising patient outcomes (Bini et al., 2022). Titanium and its alloys are widely used in orthopaedic implants due to their exceptional mechanical strength, biocompatibility, and resistance to corrosion. However, challenges such as biofilm formation, bacterial colonization, and inflammatory responses remain significant obstacles to their clinical success (Bini et al., 2022; Bodaghi et al., 2019; Chen et al., 2019; Costerton et al., 1999). Biofilms formed by pathogens such as *Staphylococcus aureus*, *Staphylococcus epidermidis*, and *Pseudomonas aeruginosa* are particularly problematic, as they confer bacterial resistance to antibiotics and immune responses, often requiring implant removal to resolve infections (Costerton et al., 1999; Donlan and Costerton, 2002). Studies have shown that bacteria within biofilms exhibit up to 1,000-fold higher resistance to antibiotics than planktonic cells, emphasizing the need for innovative solutions to prevent and mitigate infections (Donlan and Costerton, 2002; El-Sayegh et al., 2020; Geetha et al., 2019; Geetha et al., 2009). To address these challenges, surface modifications and advanced coatings have emerged as promising strategies to enhance the performance of titanium implants. Bioactive coatings, including ceramic and composite materials, are being explored for their ability to improve osseointegration and reduce the risk of bacterial infections (Gristina, 1987; Hench, 1998; Kim et al., 2022). Ceramic coatings, in particular, have demonstrated significant potential in promoting bone integration by providing bioactive surfaces that enhance cell adhesion and tissue regeneration (Geetha et al., 2019). However, optimizing coating compositions to balance mechanical stability, biocompatibility, and antimicrobial properties remains a critical challenge. In this study, we propose the development of a novel bio-ceramic composite coating for titanium implants, incorporating beta-tricalcium phosphate (β-TCP), pectin, gelatine, and polyvinylpyrrolidone (PVP). β-TCP is a recognized osteoconductive material that mimics the mineral phase of bone, facilitating cell proliferation and bone regeneration (Geetha et al., 2019; Li et al., 2019; El-Sayegh et al., 2020). Pectin, a natural polysaccharide, improves the mechanical properties of the coating while enhancing its hydrophilic and biodegradable nature, making it ideal for controlled nutrient release (Geetha et al., 2009; Li et al., 2021). Gelatine, a collagen-derived protein, supports osteoinductive and calcium absorption, promoting cell attachment and differentiation (Gristina, 1987; Hench, 1998). polyvinylpyrrolidone (PVP) provides structural stability and facilitates the controlled release of bioactive compounds, enhancing antibacterial and anti-inflammatory properties (Lin et al., 2019; Li et al., 2022). This research aims to evaluate the proposed coating's stability, uniformity, antibacterial efficacy, and its potential to support bone cell regeneration. By addressing the limitations of current coatings and contributing new insights into composite material engineering, we hope to improve the performance and longevity of titanium-based implants, ultimately enhancing patient outcomes.

2 Materials and methodology

2.1 Chemicals used

All chemicals of analytical grade used in this research were purchased from Merck.

2.2 Synthesis of the coating material

The bio-ceramic composite coating substance was prepared using a titrative (wet chemical) method, following the standard procedure described by Joseph Louis Gay-Lussac in 1828. The composite coating substance was prepared using the biomaterials beta-tricalcium phosphate, pectin, polyvinylpyrrolidone (PVP), and gelatine (purchased from Sigma Aldrich) in the ratio of 2:1:0.5:1.

Briefly, 1.0 g of gelatine was dissolved at an optimal temperature of 60°C in 99% double-distilled water and 0.5% glacial acetic acid. Subsequently, 0.5 g of polyvinylpyrrolidone (PVP) and 1.0 g of pectin were added to the gelatine solution at 60°C to form a mixture. Then, 2.0 g of beta-tricalcium phosphate was added, and the mixture was thoroughly agitated for 2 hours to form a dense, white jelly-like solution. The sample underwent dip coating using a 12 mm cortical titanium bone screw. The dip coating process was carried out three times to achieve an appropriate coating on the screw (Figure 1). For future research, the composite-coated sample was kept in a glass bottle under sterile conditions. The composite coating substance was synthesized using a titrative technique. This coating mixture was applied to the bone screw, with its effectiveness depending on several factors, including high crystallinity in the coating, good metal-ceramic adhesion, control over coating thickness, and its ability to adhere to complex and porous shapes. A specialized dip-coating device (Figure 2) was used to carry out the coating process electronically, with a constant dipping and withdrawal rate of 1 mm/s. The coated substrate was then heated to 40°C in an oven before being oven-dried for an hour at 130°C to form a white coating layer.

2.3 Composite coating substance

A composite coating for bone implants is an artificial substance applied to bone implants to heal the surrounding tissues of injured or damaged sites. Beta-tricalcium phosphate (β-TCP) is a commonly used and potent artificial bone substitute. In addition to being osteoconductive, it is also osteoinductive. These characteristics, along with its cell-mediated resorption, allow for full bone defect regeneration. Gelatine, which contains lysine, promotes bone strength and enhances calcium absorption, reducing the risk of bone loss. Due to these properties, supplements containing gelatine may lower the risk of osteoporosis or bone weakening. Various methods have been developed to produce composite coatings for bone tissue engineering applications using biomaterials such as pectin, gelatine, and polyvinylpyrrolidone (PVP) in various combinations.

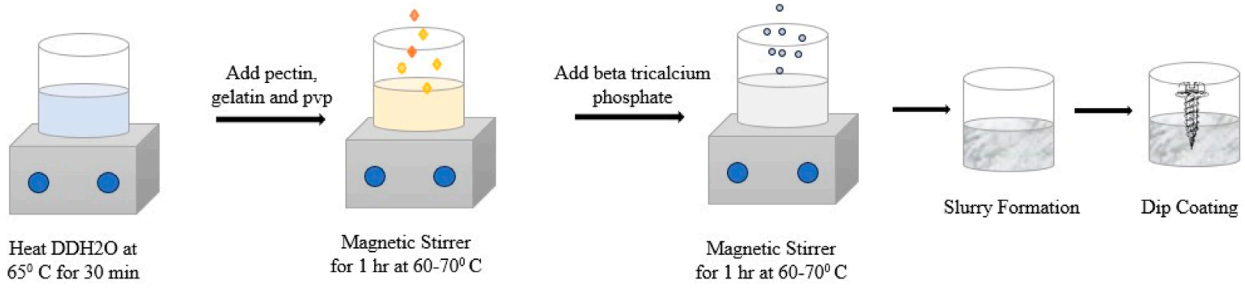

FIGURE 1
Show the flow diagram of the titration method.

FIGURE 2
Titanium cortical bone screw after dip coating ("Photograph courtesy of Author: Geetha Balasubramani. Copyright 2024").

Table 1 illustrates the six samples (H1, H2, H3, H4, H5, and H6) that were prepared using a titrative approach to standardize the composite coating substance. The samples had varying ratios of pectin, gelatine, polyvinylpyrrolidone (PVP), and beta-tricalcium phosphate. Among the composite samples used, samples H5 and H6 had an ideal layer around the bone implant, unlike the other coating combinations. Therefore, it was determined that the sample ratio of H5 and H6 was the standard, optimal combination to formulate a composite that had excellent adhesion and ideal layering around the bone screw. Titanium screws, are widely used in orthopaedic applications due to their excellent biocompatibility, corrosion resistance, and mechanical strength (Lindsey et al., 1996; Donlan and Costerton, 2002).

However, implant-associated infections (IAIs) pose a significant challenge, with infection rates ranging from 1%–5% in elective surgeries to as high as 30% in trauma-related open fractures (Ma et al., 2018; Sloan et al., 2021). Bacteria such as *Staphylococcus aureus*, *Staphylococcus* epidermidis, and *Pseudomonas aeruginosa* often colonize these implants, forming biofilms that increase bacterial resistance by up to 1,000-fold (Chen et al., 2019). Biofilm-associated infections can cause chronic inflammation, implant loosening, and bone resorption (osteolysis), necessitating revision surgeries (Travis et al., 2013; Bodaghi et al., 2019). Despite these challenges, titanium screws remain a cost-effective option for initial testing, offering a platform to refine implant technologies before scaling to larger applications like titanium plates (Geetha et al., 2019; Yang et al., 2021). Additional characterization investigations were conducted on the H6 sample, identified as the optimal formulation. Using dip coating technology, a composite coating layer with a thickness of 1–3 μm was successfully achieved. The coating demonstrated uniform interaction between the implant and the composite material, providing adequate mechanical stability and support for bone regrowth. Additionally, the composite layer offered structural support for surrounding bone cells, enhancing their development and promoting tissue regeneration. The standardized ratio for the composite preparation is presented in Table 1.

2.4 Antibacterial activity test

According to National Committee for Clinical Laboratory Standards (NCCLS) (1993), the antibacterial properties of the composite were investigated using the agar well-diffusion method

TABLE 1 Standardization ratio of synthesized composite.

S. No	β – Tricalcium phosphate (g)	Pectin (g)	Polyvinylpyrrolidone (PVP) (g)	Gelatine (g)	Results
H1	1	0.5	0.5	0.5	Liquid form
H2	1.2	0.6	0.5	0.6	Liquid form
H3	1.4	0.7	0.5	0.7	Semi-viscous
H4	1.6	0.8	0.5	0.8	Semi-viscous
H5	1.8	0.9	0.5	0.9	Semi Viscous
H6	2.0	1.0	0.5	1.0	Semi Viscous

Each ratio of composite preparation was performed three times.

on Mueller-Hinton agar (MHA) plates. The Mueller-Hinton agar (MHA) medium was prepared with pH 7 distilled water and sterilized by autoclaving for 15 min at 121°C. The Mueller-Hinton agar (MHA) was then poured into sterile petri plates under aseptic conditions in a laminar air flow hood, allowed to cool to around 40°C, and solidified. Using a sterile cotton swab soaked with a suspension of gram-positive *Streptococcus aureus*, gram-negative *Escherichia coli*, and positive control gentamicin, an inoculum comprising 10^6 CFU/mL of each freshly prepared bacterial culture was spread on the Mueller-Hinton agar (MHA) plates (Yao et al., 2019; Soltani et al., 2020). Three wells (8 mm in diameter) were punched into the agar medium and filled with different quantities of composite samples (25 µL, 50 µL, and 100 µL) and left to diffuse at room temperature for 2 h. The culture plates were then incubated at 37°C for 24 h. After incubation, the diameter (mm) of the zone of inhibition (ZOI) was measured for each plate. The experiment's mean value and standard deviation (SD) were reported for each of the three replicates. Three different doses of *Streptococcus aureus* and *Escherichia coli* were used to test the composite's antibacterial activity (25 µL, 50 µL, and 100 µL) shown in Figure 3.

FIGURE 3
Zone of inhibition (ZOI) test on MHA plate for composite polymers for gram-positive *Streptococcus aureus* and gram-negative *Escherichia coli*.

The results show that the zone of inhibition (ZOI) for the composite against both gram-positive *Streptococcus aureus* and gram-negative *Escherichia coli* was observed shown in Figure 4. These results confirm that the prepared composite exhibits excellent antibacterial activity against both gram-positive *Streptococcus aureus* and gram-negative *Escherichia coli* (Yuan et al., 2001; Yu et al., 2018; Sun et al., 2021). However, the antibacterial efficacy of the composite is considerably higher against *Streptococcus aureus* compared to *Escherichia coli*, suggesting that our material is a promising candidate to control gram-positive organisms. The broth dilution method was used to estimate the minimum inhibitory concentration (MIC) in accordance with CLSI M07-A8. For example, 0.5 McFarland: 1.5×10^8 CFU/mL of *Streptococcus aureus* and *Escherichia coli* cultures were added to the nutrient broth containing various dilutions (10^{-1} to 10^{-7}) of the polymer composite. The lowest dose at which *Escherichia coli* and *Streptococcus aureus* cannot grow visibly is known as the polymer composite's minimum inhibitory concentration, or MIC. Using a UV-visible spectrophotometer, bacterial growth in the test tubes was detected as turbidity at 600 nm after 18 h of incubation.

The minimum inhibitory concentration (MIC) that demonstrated over 75% inhibition of bacterial growth was identified. The results of the polymer composite at concentrations of 0.75 mg/mL (range of 0.5 mg–1 mg/mL) and 0.9 mg/mL (range of 0.5 mg–1 mg/mL), respectively, showed that the growth of *Escherichia coli* and *Streptococcus aureus* was inhibited (above 75%), as shown in Figure 4. The Minimum Bactericidal Concentration (MBC) test was conducted to evaluate the bactericidal efficacy of the polymer composite against *Streptococcus aureus* and *Escherichia coli*.

Minimal bactericidal activity (MBC) is defined as the lowest concentration of a substance that kills 99.9% of the bacterial population. In this study, 50 µL samples from each Minimum Inhibitory Concentration (MIC) tube were sub-cultured onto nutrient agar plates using the spread plate method and incubated at 37°C for 24 h. The experiments were performed in triplicates, and the results were reported as mean ± standard deviation. As illustrated in Figure 5A, B, the polymer composite at a concentration of 1 mg/mL (10^{-3}) completely eradicated both *S. aureus* and *E. coli*,

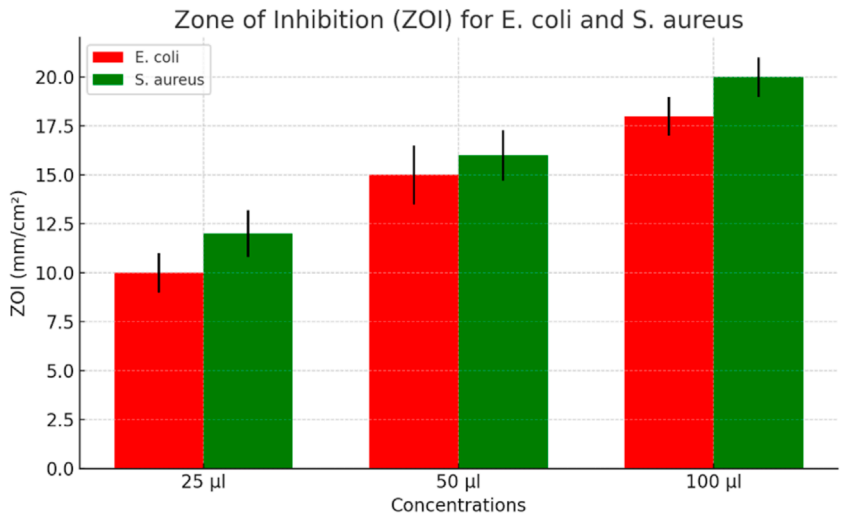

FIGURE 4
Zone of inhibition (ZOI) measurement for composite polymers.

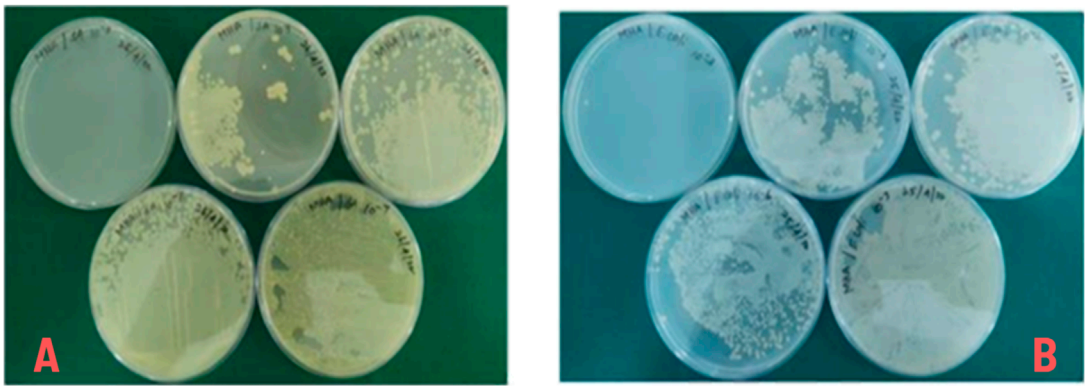

FIGURE 5
(A) Minimal bactericidal activity (MBC) of composite polymers for *Streptococcus aureus*, **(B)** Minimal bactericidal activity (MBC) of composite polymers for *Escherichia coli*.

confirming its strong bactericidal properties. Notably, the observed Minimal bactericidal activity (MBC) values were nearly identical to their respective Minimum Inhibitory Concentration (MIC) values for both species, indicating a close correlation between the inhibitory and bactericidal activity of the composite. This suggests that the composite requires minimal concentrations to exert effective bactericidal action, reducing the potential for bacterial regrowth. The bactericidal activity is attributed to the composite's ability to disrupt bacterial cell membranes, thereby preventing biofilm formation and bacterial colonization. These findings demonstrate the polymer composite's potential for biomedical applications, particularly in preventing implant-associated infections, while highlighting its reproducibility and effectiveness.

2.5 Characterization of composite coated screw

The morphology of the composite-coated sample was examined under scanning electron microscopy (Model: SEM-SUPRA 55-CARL ZEISS, Germany). The coated sample was placed in the sample grid and allowed to dry under ambient conditions for scanning electron microscopy (SEM) analysis. The functional characteristics of the composite-coated sample were examined using Fourier Transform Infrared Spectroscopy (SPECTRUM ONE: FTIR spectrometer) to identify the functional groups present in the composite-coated sample within the wavelength range of 4,000 cm-1 to 3,000 cm-1 using KBr as the standard.

2.6 *In vitro* biodegradation testing

The biodegradation testing was performed according to ISO 10993–14, "Biological evaluation of medical devices–Part 14: Identification and quantification of degradation products from ceramics." It was performed in duplicates at different pH values. To assess the peel-off of the composite from the coated screw, a composite coating stability study was performed. Briefly, the composite-coated screw was incubated in two different buffer solutions, namely, acetate buffer (pH 5.5) and phosphate buffer (pH 7.4), with two different time points (3 days) to estimate the coating stability.

$$\text{Weight loss}(\%) = \left[\left(W_o - W_t\right)/W_o\right] \times 100$$

The biodegradation tests were conducted at different time intervals (from 1 h to 3 days). The sample weight was measured before immersion in the buffer solution (W_o) and after degradation (W_t), calculated using the above formula. After the respective treatment periods in different buffer solutions, the screw was dried and analysed using scanning electron microscopy (SEM) (Manzoor et al., 2021; Zheng et al., 2021).

2.7 Anti-inflammatory study (inhibition of albumin denaturation assay)

A reaction mixture (5 mL) was incubated for 15 min at 37°C in a biochemical oxygen demand (BOD) incubator. It contained 0.2 mL of egg albumin (from a fresh hen's egg), 2.8 mL of Phosphate Buffer Saline (PBS) (pH 6.4), and a few mL of test samples at different concentrations (100 µg/mL, 200 µg/mL, 400 µg/mL, and 800 µg/mL). After 5 min of heating to 70°C, a comparable volume of H_2O was used as a control. Non-steroidal anti-inflammatory drugs (NSAID) was employed as a reference medication at doses of 100 µg/mL, 200 µg/mL, 400 µg/mL, and 800 µg/mL and treated similarly to determine absorbance. The percentage of protein denaturation inhibition was computed using:

$$\text{Percentage protection} = 100 - \left(V_t\,\text{sample}/V_c\,\text{control}\right) \times 100$$

where V_c is the absorbance of the control sample and V_t is the absorbance of the test sample. Plotting the percentage inhibition against treatment concentration allowed for the determination of the drug concentration for 50% inhibition from the dose-response curve.

3 Results

Tissue engineering is an emerging and multidisciplinary field aiming to develop biological substitutes to repair, replace, or regenerate inadequate tissues (Noroozi et al., 2020). The composite coating consisting of polymeric biomaterials must be biocompatible and biodegradable when implanted in the human body. They should be absorbable by human tissue and adhere to surrounding tissues with an adequate implant interface (Noroozi et al., 2020; Parada et al., 2017). Researchers have developed a composite layer for the implant's surrounding bone cell contact using various technologies. Both natural and synthetic biomaterials have been used to prepare composite coatings for tissue engineering (Zhou et al., 2017; Bodaghi et al., 2019).

3.1 Morphological characterization

Scanning Electron Microscope (SEM) images of the composite-coated sample showed a homogeneous nature of the coating at different magnifications, as shown in Figure 6. The diameter of the cortical screw was 6 mm, and the length was approximately 12 mm. Figure 6A shows the sharp edges and rough surface of the uncoated screw. Figure 6B Scanning Electron Microscope (SEM) micrographs show that the biomaterial polymer layer on the screw eliminates sharp edges and the rough surface. The biomaterial polymer coating was well adapted to the metal substrate.

Energy Dispersive X-ray (EDX) analysis of uncoated screws (Figure 7A, B) confirmed the presence of highly inorganic materials: 44% titanium, 4% aluminium, 1.8% vanadium, and 0.6% silicon. Since Scanning Electron Microscope (SEM) and Energy Dispersive X-ray (EDX) were done together, the Energy Dispersive X-ray (EDX) results of coated screws (Figure 7A, B) confirmed the uptake of different organic materials: 16% calcium, 1.6% copper, 43% carbon, and 3.9% phosphorus were the main components of the polymer.

3.2 Functional characterization

The chemical composition of the composite coating was analysed by attenuated total reflectance FTIR (Fourier transform infrared spectroscopy) (ATR-FTIR) (Bruker, ALPHA II Compact) in the spectral region of 4,000–400 cm^{-1} wavelength with 4 cm^{-1} resolution at total scan of (Yang et al., 2020). The Fourier transform infrared spectroscopy (FTIR) spectrum of the composite is shown in Figure 8. The broad stretching vibration was observed between 3,200–3,400 cm^{-1}, which was attributed to aromatic O-H stretching vibration of composite coating. A similar peak was observed by (Zimmerli et al., 2004; Liu et al., 2018) for pectin. The characteristic transmittance peaks of the composite were observed at 1,277 cm^{-1} (aromatic C-O stretching), 1,422 cm^{-1} (aromatic C-H stretching), 1,650 cm^{-1} (aromatic C=O stretching), and 2,099 cm^{-1} (aromatic C-H_2 stretching), as observed by (Liu et al., 2020). The spectral band at 576 cm^{-1} was noted and attributed to the characteristic spectral band of the PO_4^{2-} functional group of tricalcium phosphates, a similar peak observed by (Parada et al., 2020; Zou et al., 2021).

According to (Bodaghi et al., 2019), the vibration of the phosphate group is responsible for the unique peak bands that calcium phosphate exhibits at 1,041 cm^{-1} and 603.96 cm^{-1}. From the intense infrared absorption bands at 576 cm^{-1} to 600 cm^{-1} and from 1,000 cm^{-1} to 1,500 cm^{-1}, the phosphate group with a double-bonded group of PO_4 is shown in Figure 8. Calcium phosphate's Fourier transform infrared spectroscopy (FTIR) absorption band is visible between 600 and 1,005 cm^{-1} (Parada et al., 2020). However, the present study reveals that the amide group C=O bending hydrogen bond in the IR spectra band is present in both pectin and gelatine (Schneider et al., 2011). Polyvinylpyrrolidone (PVP)

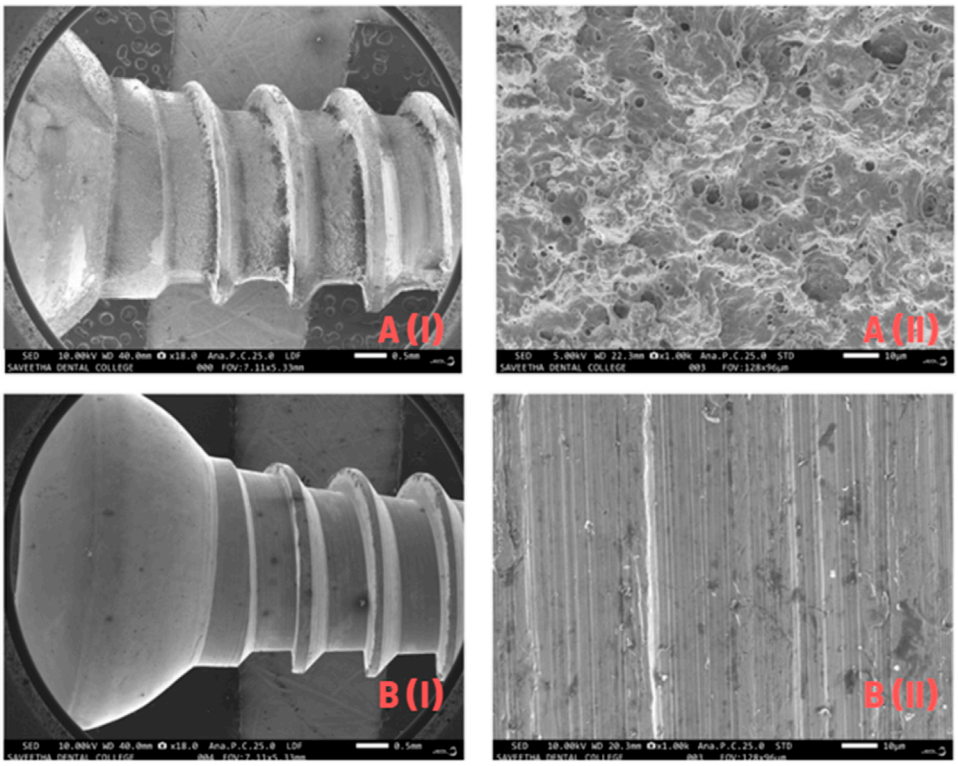

FIGURE 6
(A) Scanning Electron Microscope (SEM) analysis of Titanium screw before coating, **(B)** Scanning Electron Microscope (SEM) analysis of coated Titanium screw after coating.

and pectin exhibit biodegradable and biocompatible biopolymer characteristics within the 600 cm^{-1} to 1,650 cm^{-1} range and have been employed for numerous biological purposes. The substrate's macromolecular and micromolecular structures, which include a multitude of intermolecular interactions, explain why the peak bands are often vast.

3.3 *In-vitro* bio-degradation studies

Figure 9 illustrates the Field-emission scanning electron microscope (FE-SEM) image of uncoated screws and composite-coated screws at two different magnifications. The uncoated screw exhibited sharp blades and edges. After coating, a layer growth over the screw is visible, captured through Field-emission scanning electron microscope (FE-SEM). The coated screw was incubated at different pH levels (acetate buffer-5.5 and phosphate buffer-7.5) and two different time points (1st and 3rd day) to estimate the coating stability. The Field-emission scanning electron microscope (FE-SEM) image shows the stability nature of the composite coating on the screw (Figure 9). Samples treated at pH 5.5 showed more dominant degradation than other samples, likely due to the acidic nature of the treatments (Sloan et al., 2021). Acids tend to, etch surfaces. Screws soaked at pH 7.4 demonstrated better coating adherence on the internal structures (10 μm), but this adherence was reduced on the third day. Similarly, pH 5.5 treated screws showed lines indicating the removal of coated material over the surface. Samples treated at pH 5.5 explained the sharp natural structure of the screw compared to other samples, suggesting better coating stability at pH 7.4. The composite coating takes 2–3 months to degrade while bone cells adhere to the implant.

3.4 Biomechanical analysis of composite coating

The biomechanical performance of composite-coated screws was evaluated using finite element analysis (FEA) through Analysis System (ANSYS) software, coupled with precise measurements of the coating thickness obtained via Scanning Electron Microscopy (SEM). The Scanning Electron Microscopy (SEM) analysis provided the exact thickness of the composite coating, which was subsequently integrated into the 3D model of the screw for accurate stress and strain simulation. The simulation was designed to replicate physiological loading conditions, particularly a compression force of 27 N, corresponding to the weight of a 3 kg rat model (Figure 10). This load represents the biomechanical forces exerted on the coated screw during functional use. Material properties such as elastic modulus, yield strength, and Poisson's ratio for both the screw and the composite coating were incorporated into the model. Boundary conditions were applied to mimic the constraints of the bone-screw interface, ensuring realistic stress

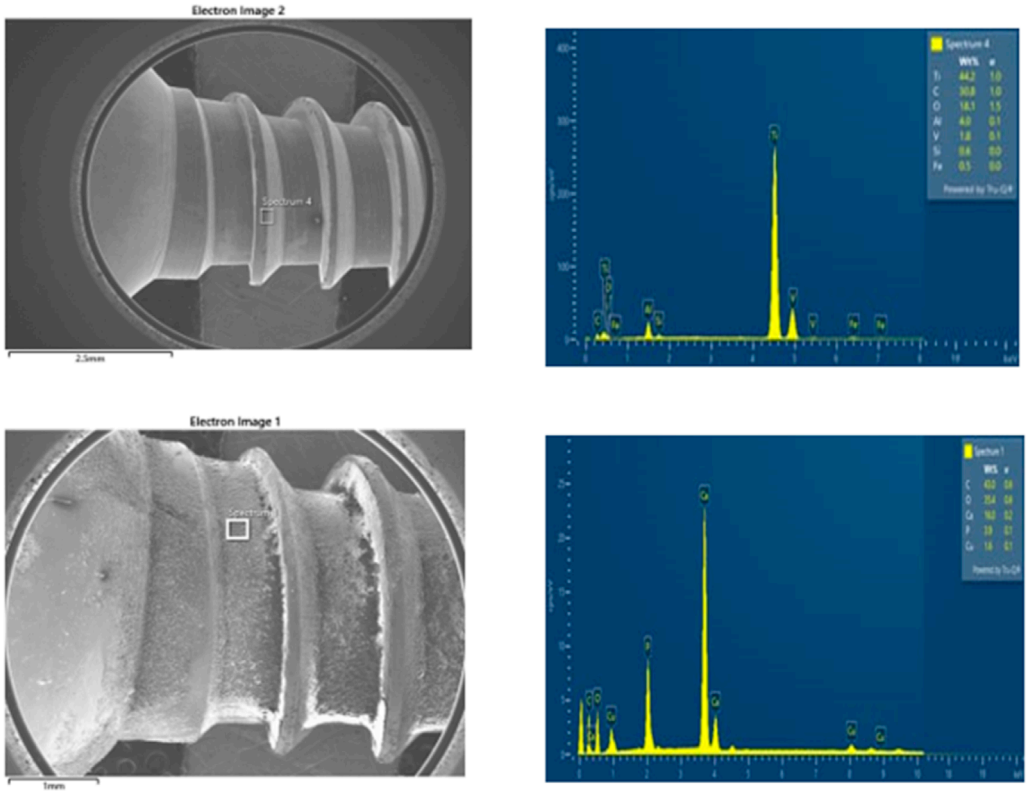

FIGURE 7
(A, B) Energy Dispersive X-ray EDX analysis of non-coated and coated Titanium screw.

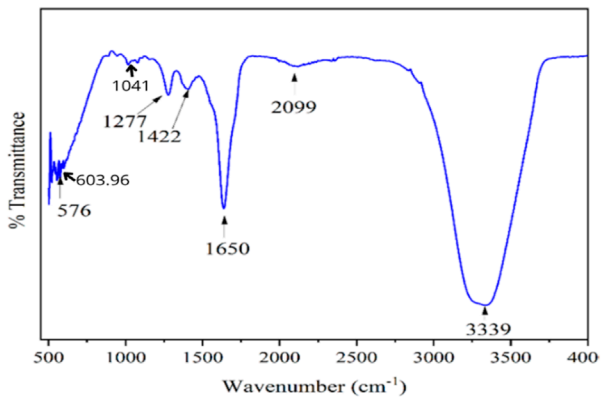

FIGURE 8
Fourier transform infrared spectroscopy graph for the coating material sample.

distribution. The simulation results highlighted the stress and strain behaviour of the coated screw under loading, differentiating between elastic and plastic deformation thresholds. Stress distribution analysis revealed effective segmentation of stress across the screw surface, reducing localized stress concentrations that could lead to coating failure. The deformation of the coating under load demonstrated its capacity to maintain structural integrity within the elastic range, as evidenced by a maximum stress tolerance of 27 N. The displacement analysis provided insights into the relative movement of the coating and screw without indicating significant material stretching or failure. These findings suggest that the composite coating enhances the biomechanical stability of the screw, supporting its application in high-stress environments. The results also validate the coating's potential to withstand physiological forces without compromising adhesion or durability, which is critical for long-term implant performance.

Furthermore, the finite element analysis (FEA) model serves as a predictive tool for understanding how varying coating compositions or thicknesses might influence mechanical behaviour under different loading conditions. This approach underscores the importance of integrating experimental data, such as Scanning Electron Microscopy (SEM) measurements, with computational analysis to optimize implant design. Overall, the biomechanical study confirms that the composite coating is a robust and reliable solution for improving the performance and longevity of orthopaedic implants. These findings align with previous studies demonstrating the utility of advanced coatings in enhancing implant durability and reducing stress-related complications (Donlan and Costerton, 2002; Geetha et al., 2019; Geetha et al., 2009). By combining Scanning Electron Microscopy (SEM) characterization and finite element analysis (FEA) simulation, this study provides a comprehensive understanding of the coating's mechanical behaviour and offers a foundation for future research in implant optimization.

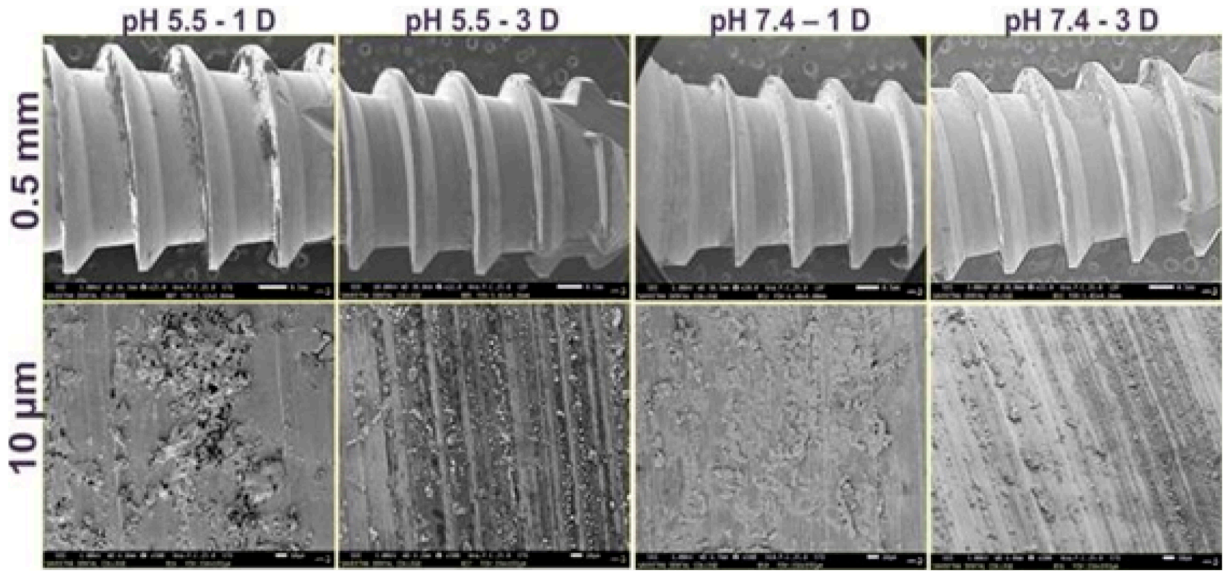

FIGURE 9
Morphological evaluation of polymer-coated screws after exposure to buffer solutions with different pH (5.5 and 7.4) at different time points (1 and 3 days).

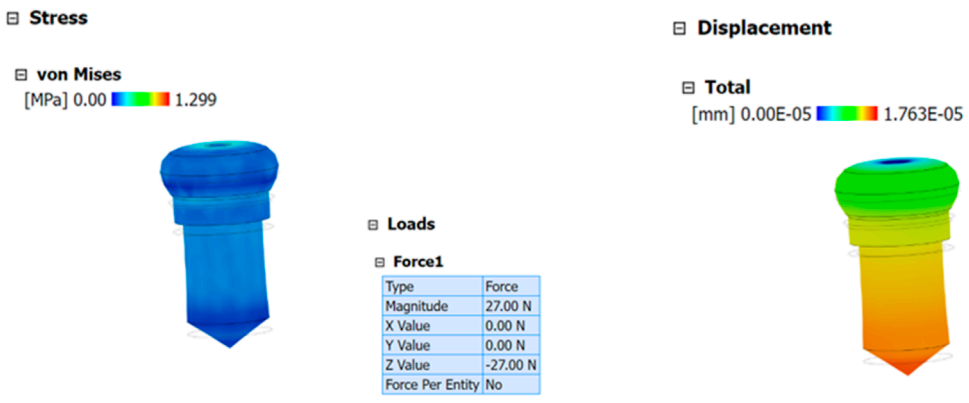

FIGURE 10
Mechanical stress and displacement simulation using AutoCAD.

3.5 Anti-inflammatory assessment

The composite coating developed for orthopaedic implants significantly contributes to reducing inflammation and preventing bacterial infections, both of which can impair tissue metabolism. The anti-inflammatory properties of the composite were assessed using the egg albumin denaturation assay, where a maximum inhibition of 26% was achieved at 0.8 mg/mL, compared to the 65% inhibition by acetylsalicylic acid at 0.1 mg/mL (Figure 11). While the composite's inhibition percentage is moderate, it effectively reduces protein denaturation, a key factor in inflammation, creating a favourable environment for tissue regeneration. This reduction in inflammation promotes better cell adhesion and enhances tissue metabolism during the healing process. Bacterial infections often accompany orthopaedic implants, leading to immune responses and complications such as osteolysis and implant loosening. The composite coating mitigates these risks by acting as a barrier to bacterial adhesion while enhancing cell proliferation. Components such as β-tricalcium phosphate (β-TCP) and gelatine play a significant role in promoting osteogenesis by supporting calcium absorption and providing a bioactive surface for bone cell growth (Yang et al., 2020).

These properties directly enhance tissue metabolism and integration with the implant. The composite's stability was evaluated under neutral pH (7.4) and acidic pH (5.5) conditions, simulating physiological and inflammatory environments, respectively. At neutral pH, the coating demonstrated excellent stability and adherence to the implant surface, supporting prolonged tissue regeneration. At acidic pH, degradation was more pronounced, suggesting the composite's vulnerability under inflammatory

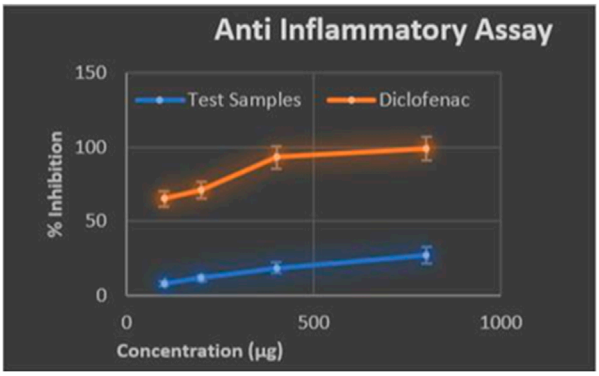

FIGURE 11
Anti-inflammatory effect of polymer composite.

conditions. However, the coating's stability in physiological pH underscores its effectiveness in supporting bone regeneration under normal conditions (Kim et al., 2022). The results indicate that the composite coating supports tissue metabolism by reducing inflammation and enhancing the osteogenic potential of implants, making it a viable material for preventing bacterial colonization and promoting cell attachment during the healing process.

4 Discussion

The morphological characterization through Scanning Electron Microscope (SEM) and Energy Dispersive X-ray (EDX) analyses demonstrated that the composite coating successfully masked the sharp edges and roughness of the titanium screw, providing a smoother surface conducive to tissue interaction. The Energy Dispersive X-ray (EDX) analysis verified the presence of calcium and phosphorus, which are crucial for osteoconduction and osteoinduction, within the coated screws. As described in Bodaghi et al. (2019), the polymer-coated screw surfaces, featuring a beta-tricalcium phosphate layer, exhibit slight flexibility while maintaining sufficient strength to establish strong interconnectivity with surrounding tissues. According to (Patel and Goyal, 2017), multiphasic calcium fiber used for composite coating preparation increases surrounding interconnectivity as fiber content increases. The morphological analysis taken together with Scanning Electron Microscope (SEM) and Energy Dispersive X-ray (EDX) demonstrated the multilayer coating of hydroxyapatite and phase-transited lysozyme (HA/PTL) on titanium implants *in vivo* and *in vitro*, as indicated by Parada et al. (2020), which suggested the presence of osteoinductive phenomena and increased biocompatibility. Composite coatings protect metal implants from bacterial infection and inflammation in the jointed region of the human body. Additionally, these coatings enhance the implants' strength, surface hardness, and anti-inflammatory properties. The functional characterization through Fourier transform infrared spectroscopy (FTIR) identified the characteristic bands of the composite components, such as the phosphate group from β-TCP and functional groups from pectin and gelatine. The composite coating developed for titanium screws exhibited a slow degradation rate of 2–3 months, which is sufficient to support osseointegration, a process where bone cells adhere to the implant surface and integrate with surrounding tissue. Osseointegration begins within 1–2 weeks post-surgery and stabilizes over 6–12 weeks, matching the coating's degradation timeline and providing temporary mechanical stability while facilitating bone regeneration (Albrektsson et al., 1981). The biomechanical analysis confirmed that the coating could withstand mechanical forces without deformation, supporting its use in load-bearing implants. This is a critical feature for orthopaedic applications, where implants must endure physical stresses during movement. The antibacterial tests showed that the composite effectively inhibited both gram-positive and gram-negative bacteria, with stronger efficacy against *Streptococcus aureus*. This suggests that the composite coating could reduce the risk of post-surgical infections, particularly from gram-positive pathogens, which are common in orthopaedic implant-related infections. Finally, the anti-inflammatory assessment, while showing moderate inhibition of albumin denaturation, indicated that the composite has potential for reducing inflammation around implants. Although the anti-inflammatory effect was lower than that of standard drugs like acetylsalicylic acid, the results are encouraging and warrant further optimization of the composite's anti-inflammatory properties. The composite coating composed of beta-tricalcium phosphate, gelatine, polyvinylpyrrolidone (PVP), and pectin-based micro and macroporous structures has showed great potential in orthopaedic applications. With a moderate rise in anti-inflammatory activity ranging from 27%–30% and excellent antibacterial activity, it is a promising choice for reducing post-implant infections. The coating's capacity to improve cell adhesion and proliferation, which is aided by beta-tricalcium phosphate, shows its potential for enhancing bone tissue regeneration and implant integration. The coating's micro and macroporous structure increased the surface-to-volume ratio, promoting better interaction with the surrounding tissues and optimal nutrient exchange to promote tissue growth. Although the preliminary results are promising, further *in-vitro* and *in-vivo* investigations are needed to optimise its anti-inflammatory qualities and validate its bone regeneration capabilities. The ongoing research intends to refine the biodegradation rate and assess the coating's long-term mechanical stability. However, this composite coating provides an adequate basis for the development of novel orthopaedic drug delivery systems and bone tissue engineering applications.

Data availability statement

The original contributions presented in the study are included in the article/supplementary material, further inquiries can be directed to the corresponding author.

Author contributions

GB: Conceptualization, Investigation, Methodology, Project administration, Resources, Supervision, Validation, Visualization, Writing–original draft, Writing–review and editing. PJ: Validation, Visualization, Writing–original draft, Writing–review and editing, Investigation, Methodology, Supervision. PPJ: Validation, Visualization, Writing–original draft, Writing–review and editing.

Funding

The author(s) declare that no financial support was received for the research, authorship, and/or publication of this article.

Acknowledgments

We thank Sathyabama Institute of Science and Technology and Medcuore Medical Solutions Private Limited for providing the infrastructure to carry out the project. Veltech and DR SR R&D Institute of Science and Technology and Material Research Center Saveetha Dental College for providing analytical support for our work.

Conflict of interest

Author JPP was employed by MedCuore Medical Solutions Private Limited.

The remaining authors declare that the research was conducted in the absence of any commercial or financial relationships that could be construed as a potential conflict of interest.

Generative AI statement

The author(s) declare that no Generative AI was used in the creation of this manuscript.

Publisher's note

All claims expressed in this article are solely those of the authors and do not necessarily represent those of their affiliated organizations, or those of the publisher, the editors and the reviewers. Any product that may be evaluated in this article, or claim that may be made by its manufacturer, is not guaranteed or endorsed by the publisher.

References

Albrektsson, T., Brånemark, P. I., Hansson, H. A., and Lindström, J. (1981). Osseointegrated titanium implants:Requirements for Ensuring a long-lasting, direct bone-to-implant Anchorage in man. *Acta Orthop. Scand.* 52 (2), 155–170. doi:10.3109/17453678108991776

Bello, A. B., Kim, D., Kim, D., Park, H., and Lee, S. H. (2020). Gelatin-based hydrogels: a versatile platform for tissue engineering applications. *Tissue Eng. Regen. Med.* 17 (5), 719–748.

Bini, S. A., Mahoney, O. M., and Padgett, D. E. (2022). The evolution of knee replacement technologies: a historical review. *J. Arthroplasty* 37 (4), S1–S8.

Bodaghi, M., Noroozi, R., Zolfagharian, A., Fotouhi, M., and Norouzi, S. (2019). 4D printing self-morphing structures. *Materials* 12 (8), 1353. doi:10.3390/ma12081353

Chen, C.-Y., Rao, S.-S., Tan, Y.-J., Luo, M.-J., Hu, X.-K., Yin, H., et al. (2019). Extracellular vesicles from human urine-derived stem cells prevent osteoporosis by transferring CTHRC1 and OPG. *Bone Res.* 7 (1), 18. doi:10.1038/s41413-019-0056-9

Costerton, J. W., Stewart, P. S., and Greenberg, E. P. (1999). Bacterial biofilms: a common cause of persistent infections. *Science* 284 (5418), 1318–1322. doi:10.1126/science.284.5418.1318

Donlan, R. M., and Costerton, J. W. (2002). Biofilms: survival mechanisms of clinically relevant microorganisms. *Clin. Microbiol. Rev.* 15 (2), 167–193. doi:10.1128/cmr.15.2.167-193.2002

El-Sayegh, S., Romdhane, L., and Manjikian, S. (2020). A critical review of 3D printing in construction: benefits, challenges, and risks. *Archives Civ. Mech. Eng.* 20 (2), 34. doi:10.1007/s43452-020-00038-w

Geetha, B., Premkumar, J., Pradeep, J. P., and Krishnakumar, S. (2019). Synthesis and characterization of bioscaffolds using freeze drying technique for bone regeneration. *Biocatal. Agric. Biotechnol.* 20, 101184. doi:10.1016/j.bcab.2019.101184

Geetha, M., Singh, A. K., Asokamani, R., and Gogia, A. K. (2009). Ti based biomaterials, the ultimate choice for orthopaedic implants – a review. *Prog. Mater. Sci.* 54 (3), 397–425. doi:10.1016/j.pmatsci.2008.06.004

Gristina, A. G. (1987). Biomaterial-centered infection: microbial adhesion versus tissue integration. *Science* 237 (4822), 1588–1595. doi:10.1126/science.3629258

Hench, L. L. (1998). Bioceramics. *J. Am. Ceram. Soc.* 81 (7), 1705–1728. doi:10.1111/j.1151-2916.1998.tb02540.x

Kim, J., Lee, J. E., Kim, J. H., Kim, S. H., and Park, J. H. (2022). Polyvinylpyrrolidone-based coatings for orthopedic implants: mechanical properties and antibacterial efficacy. *Mater. Sci. and Eng. C* 140 (3), 112519.

Li, H., Ye, W., Liu, X., and Tang, L. (2022). Advances in antibacterial coatings for orthopedic implants: balancing infection control and osseointegration. *Acta Biomater.* 10 (6), 1056–1070.

Li, W., Liu, X., Deng, Z., Chen, Y., Yu, Q., Tang, W., et al. (2019). Tough bonding, on-demand debonding, and facile rebonding between hydrogels and diverse metal surfaces. *Adv. Mater.* 31, e1904732. doi:10.1002/adma.201904732

Li, Z., Du, T., Ruan, C., and Niu, X. (2021). Bioinspired mineralized collagen scaffolds for bone tissue engineering. *Bioact. Mater.* 6 (5), 1491–1511. doi:10.1016/j.bioactmat.2020.11.004

Lin, S., Liu, X., Liu, J., Yuk, H., Loh, H.-C., Parada, G. A., et al. (2019). Anti-fatigue-fracture hydrogels. *Sci. Adv.* 5 (1), eaau8528. doi:10.1126/sciadv.aau8528

Lindsey, W. H., Ogle, R. C., Morgan, R. F., Cantrell, R. W., and Sweeney, T. M. (1996). Nasal reconstruction using an osteoconductive collagen gel matrix. *Archives Otolaryngology - Head Neck Surg.* 122 (1), 37–40. doi:10.1001/archotol.1996.01890130031004

Liu, J., Qu, S., Suo, Z., and Yang, W. (2020). Functional hydrogel coatings. *Natl. Sci. Rev.* 8 (2), nwaa254. doi:10.1093/nsr/nwaa254

Liu, Q., Nian, G., Yang, C., Qu, S., and Suo, Z. (2018). Bonding dissimilar polymer networks in various manufacturing processes. *Nat. Commun.* 9 (1), 846. doi:10.1038/s41467-018-03269-x

Ma, S., Yan, C., Cai, M., Yang, J., Wang, X., Zhou, F., et al. (2018). Continuous surface polymerization via fe(ii)-mediated redox reaction for thick hydrogel coatings on versatile substrates. *Adv. Mater.* 30, e1803371. doi:10.1002/adma.201803371

Manzoor, F., Golbang, A., Jindal, S., Dixon, D., McIlhagger, A., Harkin-Jones, E., et al. (2021). 3D printed peek/ha composites for bone tissue engineering applications: effect of material formulation on mechanical performance and bioactive potential. *J. Mech. Behav. Biomed. Mater.* 121, 104601. doi:10.1016/j.jmbbm.2021.104601

Noroozi, R., Bodaghi, M., Jafari, H., Zolfagharian, A., and Fotouhi, M. (2020). Shape-adaptive metastructures with variable bandgap regions by 4D printing. *Polymers* 12 (3), 519. doi:10.3390/polym12030519

Parada, G., Yu, Y., Riley, W., Lojovich, S., Tshikudi, D., Ling, Q., et al. (2020). Ultrathin and robust hydrogel coatings on cardiovascular medical devices to mitigate thromboembolic and infectious complications. *Adv. Healthc. Mater.* 9 (20), 2001116. doi:10.1002/adhm.202001116

Parada, G. A., Yuk, H., Liu, X., Hsieh, A. J., and Zhao, X. (2017). Impermeable robust hydrogels via hybrid lamination. *Adv. Healthc. Mater.* 6 (19), 1700520. doi:10.1002/adhm.201700520

Patel, A., and Goyal, R. K. (2017). Applications of pectin in pharmaceutical formulations. *Expert Opin. Drug Deliv.* 14 (5), 1–15.

Schneider, M. H., Tran, Y., and Tabeling, P. (2011). Benzophenone absorption and diffusion in poly(dimethylsiloxane) and its role in graft photo-polymerization for surface modification. *Langmuir* 27 (3), 1232–1240. doi:10.1021/la103345k

Sloan, M., Premkumar, A., and Sheth, N. P. (2021). Projected volume of primary total joint arthroplasty in the U.S., 2030 to 2060. *JBJS* 103 (4), 1–9.

Soltani, A., Noroozi, R., Bodaghi, M., Zolfagharian, A., and Hedayati, R. (2020). 3D printing on-water sports boards with bio-inspired core designs. *Polymers* 12 (1), 250. doi:10.3390/polym12010250

Sun, T., Meng, C., Ding, Q., Yu, K., Zhang, X., Zhang, W., et al. (2021). *In situ* bone regeneration with sequential delivery of aptamer and BMP2 from an ECM-based

scaffold fabricated by cryogenic free-form extrusion. *Bioact. Mater.* 6 (11), 4163–4175. doi:10.1016/j.bioactmat.2021.04.013

Travis, J. K. 1, Malda, J., Sah, R. L., and Hutmacher, D. W. (2013). Tissue engineering of articular cartilage. *Articul. Cartil.*, 165–248. doi:10.1201/b14183-5

Yang, X. X., Yang, C. H., Liu, J. J., Yao, X., and Suo, Z. G. (2020). Topological prime. *Sci. China Technol. Sci.* 63 (7), 1314–1322. doi:10.1007/s11431-019-1498-y

Yang, Z., He, Y., Liao, S., Ma, Y., Tao, X., and Wang, Y. (2021). Renatured hydrogel painting. *Sci. Adv.* 7 (23), eabf9117. doi:10.1126/sciadv.abf9117

Yao, X., Liu, J., Yang, C., Yang, X., Wei, J., Xia, Y., et al. (2019). Hydrogel paint. *Adv. Mater.* 31 (39), 1903062. doi:10.1002/adma.201903062

Yu, Y., Yuk, H., Parada, G. A., Wu, Y., Liu, X., Nabzdyk, C. S., et al. (2018). Multifunctional "hydrogel skins" on diverse polymers with arbitrary shapes. *Adv. Mater.* 31 (7), 1807101. doi:10.1002/adma.201807101

Yuan, H., Fernandes, H., Habibovic, P., de Boer, J., Barradas, A. M., and van Blitterswijk, C. A. (2001). Osteoinductive ceramics as a synthetic alternative to autologous bone grafting. *PNAS* 98 (5), 13640–13645.

Zheng, J., Kang, J., Sun, C., Yang, C., Wang, L., and Li, D. (2021). Effects of printing path and material components on mechanical properties of 3D-printed polyether-ether-ketone/hydroxyapatite composites. *J. Mech. Behav. Biomed. Mater.* 118, 104475. doi:10.1016/j.jmbbm.2021.104475

Zhou, Y., Zhang, M., Guo, Z., Miao, L., Han, S.-T., Wang, Z., et al. (2017). Recent advances in black phosphorus-based photonics, electronics, sensors and Energy Devices. *Mater. Horizons* 4 (6), 997–1019. doi:10.1039/c7mh00543a

Zimmerli, W., Trampuz, A., and Ochsner, P. E. (2004). Prosthetic-joint infections. *N. Engl. J. Med.* 351 (16), 1645–1654. doi:10.1056/nejmra040181

Zou, Z., Wang, L., Zhou, Z., Sun, Q., Liu, D., Chen, Y., et al. (2021). Simultaneous incorporation of PTH (1–34) and nano-hydroxyapatite into chitosan/alginate hydrogels for efficient bone regeneration. *Bioact. Mater.* 6 (6), 1839–1851. doi:10.1016/j.bioactmat.2020.11.021